

# MOTION INVERSION FOR VIDEO CUSTOMIZATION

Anonymous authors

Paper under double-blind review



Figure 1: **Applications of the proposed Motion Embeddings for customized video generation.** Our method supports a wide range of motion types, including various camera movements and object motions. In each example, the first row shows the source video, while the second row shows the output. Please refer to the supplementary videos for clearer visualization.

## ABSTRACT

In this work, we present a novel approach for motion customization in video generation, addressing the widespread gap in the exploration of motion representation within video generative models. Recognizing the unique challenges posed by the spatiotemporal nature of video, our method introduces **Motion Embeddings**, a set of explicit, temporally coherent embeddings derived from a given video. These embeddings are designed to integrate seamlessly with the temporal transformer modules of video diffusion models, modulating self-attention computations across frames without compromising spatial integrity. Our approach provides a compact and efficient solution to motion representation, utilizing two types of embeddings: a Motion Query-Key Embedding to modulate the temporal attention map and a Motion Value Embedding to modulate the attention values. Additionally, we introduce an inference strategy that excludes spatial dimensions from the Motion Query-Key Embedding and applies a debias operation to the Motion Value Em-

054 bedding, both designed to debias appearance and ensure the embeddings focus  
 055 solely on motion. Our contributions include the introduction of a tailored motion  
 056 embedding for customization tasks and a demonstration of the practical advan-  
 057 tages and effectiveness of our method through extensive experiments.

## 060 1 INTRODUCTION

062 In recent years, generative models have rapidly evolved, achieving remarkable results across various  
 063 domains such as image (Rombach et al., 2022; Nichol et al., 2021; Ramesh et al., 2022; Betker  
 064 et al., 2023; Saharia et al., 2022) and video (He et al., 2022; Chen et al., 2023a; Guo et al., 2023;  
 065 Wang et al., 2023). Within the realm of imagery, customization is a popular topic, empowering  
 066 models to learn specific visual concepts from user-provided images at both the object and style  
 067 levels. These concepts are combined with the model’s extensive prior knowledge to produce diverse  
 068 and customized outcomes. The success of image customization has led to high expectations for  
 069 extending such capabilities to video generation models, which are developing rapidly and drawing  
 070 significant attention.

071 However, extending these techniques to Text-to-Video (T2V) generation introduces new challenges  
 072 due to the spatiotemporal nature of video. Unlike images, videos contain motion in addition to  
 073 appearance, making it essential to account for both. Current customization methods (Hu et al.,  
 074 2021; Mou et al., 2023; Sohn et al., 2023; Ye et al., 2023; Zhang & Agrawala, 2023; Gal et al.,  
 075 2022; Ruiz et al., 2023) primarily focus on appearance customization, neglecting motion, which is  
 076 critical in video. Motion customization deals with adapting specific movements or animations to  
 077 different objects or characters, a task complicated by the diverse shapes and dynamic changes over  
 078 time (Siarohin et al., 2019a;b; Yatim et al., 2023; Jeong et al., 2023). These methods, however, fail to  
 079 capture the dynamics of motion. For instance, textual inversion (Gal et al., 2022) learns embeddings  
 080 from images but lacks the ability to capture temporal correlations, which are essential for video  
 081 dynamics. Similarly, fine-tuning approaches like DreamBooth (Ruiz et al., 2023) and LoRA (Hu  
 082 et al., 2021) struggle to disentangle motion from appearance.

083 In this paper, we address the challenge of motion customization, focusing on the critical issue of  
 084 motion representation. The current state-of-the-art methods face several limitations: 1) Some ap-  
 085 proaches lack a clear representation of motion, as seen in Yatim et al. (2023), where motion is only  
 086 indirectly injected through loss construction and optimization at test time, leading to additional com-  
 087 putational overhead. 2) Some other methods (Jeong et al., 2023) attempt to parameterize motion as  
 088 a learnable representation, yet they fail to separate these parameters from the generative model. This  
 089 coupling compromises the generative model’s diversity after learning. 3) While there are also some  
 090 methods that attempt to separate motion representation from the generative model using techniques  
 091 like low-rank adaptation (LoRA) (Hu et al., 2021), such as in Motion Director (Zhao et al., 2023),  
 092 they lack a well-defined temporal design, limiting their effectiveness in capturing motion dynamics,  
 as evidenced by our experiments.

093 To address the aforementioned issues, we propose a novel framework for motion customization.  
 094 Our method learns explicit, temporally coherent embeddings, termed **Motion Embeddings**, from  
 095 a reference video. These embeddings are integrated into the temporal transformer modules of the  
 096 video diffusion model, modulating the self-attention across frames.

097 We introduce two types of motion embeddings: **Motion Query-Key Embedding**, which captures  
 098 global relationships between frames by influencing the temporal attention map (QK), and **Motion**  
 099 **Value Embedding**, which captures spatially varying movements across frames by modulating the  
 100 attention value (V). The Motion Query-Key Embedding excludes spatial dimensions ( $H$  and  $W$ )  
 101 to avoid capturing appearance information, as the temporal attention map inherently carries spatial  
 102 details of objects, which could entangle appearance information of the reference video and thus hin-  
 103 der motion transfer. While the Spatial-2D Motion Value Embedding may still risk capturing static  
 104 appearance information, we address this by introducing a debiasing strategy that models frame-to-  
 105 frame changes, ensuring that the embeddings primarily represent motion dynamics. This approach  
 106 is conceptually similar to techniques like optical flow, where motion is isolated by tracking changes  
 107 between frames, helping to prevent overfitting to specific appearance details and improving gener-  
 alization to novel content.

In summary, our contributions are as follows:

- We propose a novel motion representation for video generation, addressing the key challenges in motion customization.
- We design two approaches to debias appearance for this motion representation: a 1D Motion Query-Key Embedding that captures global temporal relationships, and a 2D Motion Value Embedding with a debias operation that captures spatially varying movements across frames.
- Our method is validated through extensive experiments, demonstrating its effectiveness and flexibility for integration with existing Text-to-Video frameworks.

## 2 RELATED WORK

**Text-to-Video Generation.** Text-to-Video (T2V) generation task aims to synthesize high-quality video from user-provided text prompts, which are composed of the expected appearances and motions. Previously, Generative Adversarial Networks (GANs) (Vondrick et al., 2016; Saito et al., 2017; Pan et al., 2017; Li et al., 2018; Tian et al., 2021) and Autoregressive Transformers (Yan et al., 2021; Le Moing et al., 2021; Wu et al., 2022; Hong et al., 2022) have been widely explored in this area. On the other hand, diffusion models have demonstrated powerful generation capabilities in the field of Text-to-Image (T2I) generation (Rombach et al., 2022; Nichol et al., 2021; Ramesh et al., 2022; Betker et al., 2023; Saharia et al., 2022) and have begun to extend to video generation (He et al., 2022; Chen et al., 2023a; Wang et al., 2023; He et al., 2022). Recently, several works have tried to transfer the pretrained T2I diffusion models to T2V generation models by inserting temporal layers into the image generation networks such as AnimateDiff (Guo et al., 2023), and Make-a-Video (Singer et al., 2022). These Text-to-Video (T2V) models approach frame generation as a series of image creations, integrating a temporal transformer to bolster inter-frame relationships—a notable deviation from Text-to-Image (T2I) models (He et al., 2022; Chen et al., 2023a; Wang et al., 2023; Singer et al., 2022; Zhang et al., 2023; 2024; Chen et al., 2024; cersperse, 2023). Additionally, certain approaches incorporate an extra 3D convolutional layer to enhance temporal consistency (cersperse, 2023; Wang et al., 2023). These T2V models are designed for video generation through text inputs and may encounter difficulties when needed to produce videos with customized motions.

**Video Editing.** Video editing generates video that adheres to the target prompt as well as preserves the spatial layout and motion of the input video. As the basis of video editing, image editing has achieved significant progress by manipulating the internal feature representation of prominent T2I diffusion models (Cao et al., 2023; Chefer et al., 2023; Hertz et al., 2022; Ma et al., 2023b; Tulyan et al., 2023; Patashnik et al., 2023; Bar-Tal et al., 2022; Qi et al., 2023; Liu et al., 2023). MagicEdit (Liew et al., 2023) takes use of SDEdit (Meng et al., 2021) for each video frame to conduct high-fidelity editing. Tune-A-Video (Wu et al., 2023) finetunes a T2I model on the source video and stylizes the video or replaces object categories via the fine-tuned model. Control-A-Video (Chen et al., 2023b) presents Video-ControlNet, a T2V diffusion model that generates high-quality, consistent videos with fine-grained control by incorporating spatial-temporal attention and novel noise initialization for motion coherence. TokenFlow (Geyer et al., 2023) performs frame-consistent editing by the feature replacement between the nearest neighbor of target frames and keyframes. However, these methods fall short as they just duplicate the original motion almost at pixel-level, resulting in failures when being required to require significant structural deviation from the original video.

**Video Motion Customization.** Motion customization involves generating a video that maintains the motion traits from a source video, such as direction, speed, and pose, while transforming the dynamic object to match a text prompt’s specified visual characteristics. This process is distinct from video editing (Bar-Tal et al., 2022; Chen et al., 2023b; Wu et al., 2023; Geyer et al., 2023; Liew et al., 2023; Qi et al., 2023), which typically transfers motion between similar videos within the same object category. In contrast, motion customization requires transferring motion across diverse object categories, often involving significant shape and deformation changes over time, necessitating a deep understanding of object appearance, dynamics, and scene interaction (Yatim et al., 2023; Jeong et al., 2023; Zhao et al., 2023; Ling et al., 2024; Jeong et al., 2024). Diffusion Motion Transfer (DMT) (Yatim et al., 2023) injects the motion of the reference video through the guidance of a

handcrafted loss during inference, bringing additional computation costs that could not be ignored. Video Motion Customization (VMC) (Jeong et al., 2023) encodes the motion into the parameters of a T2V model. However, finetuning the original T2V model could seriously limit the diversity of the generation model after learning the motion. Motion Director (Zhao et al., 2023) adopts LoRA (Hu et al., 2021) to embed the motion outside the T2V model. Nevertheless, the structure of LoRA limits the scalability and interpretability, as we could not easily integrate several reference motions by these methods. Other works that represent motion using parameterization (Wang et al., 2024; He et al., 2024) or trajectories (Ma et al., 2023a; Yin et al., 2023), but these approaches fall outside the scope of our discussion on reference video-based methods.

### 3 METHODOLOGY

#### 3.1 TEXT-TO-VIDEO DIFFUSION MODEL

In video diffusion models, the evolution from Text-to-Image (T2I) to Text-to-Video (T2V) models is marked by the introduction of the temporal transformer module to the basic block. While T2V models utilize **spatial convolutional layers** and **spatial transformers** in basic block for integrating image features and textual information (Rombach et al., 2022; Nichol et al., 2021; Ramesh et al., 2022; Betker et al., 2023; Saharia et al., 2022), T2V models build on this by adding the **temporal transformer** (He et al., 2022; Chen et al., 2023a; Guo et al., 2023; Wang et al., 2023). This module is key for video generation, enabling the treatment of videos as sequences of batched images. It specifically handles the inter-frame correlations through a frame-level self-attention mechanism, ensuring the temporal continuity vital for dynamic video content.

In this module, an input spatiotemporal feature tensor is provided, initially shaped as  $\mathbf{X} \in \mathbb{R}^{1 \times C \times N \times H \times W}$ , where  $C, N, H, W$  represents channels, number of frames, height, and width respectively. Batch size equals to one, and we omit the batch size dimension in our later notation for simplicity. This tensor is subsequently transformed into a feature tensor  $\mathbf{F}$ , with dimensions  $\mathbf{F} \in \mathbb{R}^{(H \times W) \times N \times C}$ . The temporal attention mechanism (TA) within this module specifically targets the  $N$  dimension, corresponding to frames.

To facilitate this operation,  $F$  is projected through three distinct linear layers to generate the Query ( $\mathbf{Q} = \mathbf{W}_q \mathbf{F}$ ), Key ( $\mathbf{K} = \mathbf{W}_k \mathbf{F}$ ), and Value ( $\mathbf{V} = \mathbf{W}_v \mathbf{F}$ ) matrices, respectively. This setup enables the execution of self-attention across the frame sequence, encapsulated by the formula:

$$\text{TA}(\mathbf{F}) = \text{softmax} \left( \frac{\mathbf{Q}\mathbf{K}^T}{\sqrt{d_k}} \right) \mathbf{V}, \quad (1)$$

where  $\mathbf{Q}$ ,  $\mathbf{K}$ , and  $\mathbf{V}$  are the query, key, and value matrices obtained from  $\mathbf{F}$ , and  $d_k$  represents the dimensionality of the key vectors, serving as a scaling factor to maintain numerical stability within the softmax function. This temporal attention mechanism allows each frame’s updated feature to gather information from other frames, enhancing the inter-frame relationships and capturing the temporal continuity essential for video generation.

#### 3.2 OUR PROPOSED METHOD

At the heart of our method for enhancing inter-frame dynamics in video models is the innovative **motion embedding** concept:

$$\begin{aligned} \mathcal{M} &= \{\mathcal{M}^{\mathcal{QK}}, \mathcal{M}^{\mathcal{V}}\}, \\ \mathcal{M}^{\mathcal{QK}} &= \{\mathbf{m}_1^{\mathcal{QK}}, \mathbf{m}_2^{\mathcal{QK}}, \dots, \mathbf{m}_L^{\mathcal{QK}}\}, \quad \text{where each } \mathbf{m}_i^{\mathcal{QK}} \in \mathbb{R}^{1 \times N \times C}, \\ \mathcal{M}^{\mathcal{V}} &= \{\mathbf{m}_1^{\mathcal{V}}, \mathbf{m}_2^{\mathcal{V}}, \dots, \mathbf{m}_L^{\mathcal{V}}\}, \quad \text{where each } \mathbf{m}_i^{\mathcal{V}} \in \mathbb{R}^{(H \times W) \times N \times C}. \end{aligned} \quad (2)$$

We have designed two distinct types of motion embeddings, each influencing different parts of the temporal attention computation. The **Motion Query-Key Embedding**  $\mathbf{m}_i^{\mathcal{QK}}$  is a learnable vector with the shape  $(1, N, C)$ , while **Motion Value Embedding**  $\mathbf{m}_i^{\mathcal{V}}$  is a learnable matrix with the shape  $(H \times W, N, C)$ . These embeddings are seamlessly integrated into the spatiotemporal feature tensor

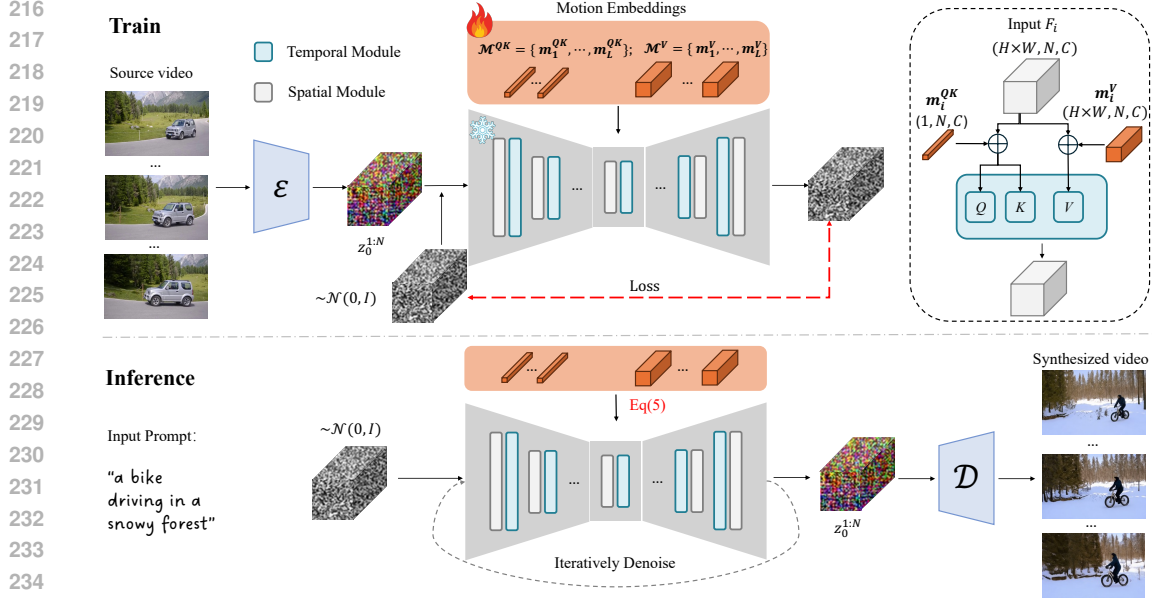


Figure 2: **Motion Inversion within T2V diffusion models.** The **top** depicts the training phase, where motion embeddings  $\mathcal{M}$  are learned by backpropagating the loss through the temporal transformer, influencing the spatiotemporal feature tensor  $\mathbf{F}$ . These embeddings are then used to modify the self-attention computations within the temporal transformer modules, ensuring enhanced inter-frame dynamics. The **bottom** shows the inference phase, where an input text prompt guides the generation of a coherent video sequence with the learned motion embeddings applied across the frames, producing a customized video output with desired motion attributes.

**F.** The variable  $L$  denotes the total number of temporal attention modules within the model. Our motion embeddings directly influence the self-attention computation as follows:

$$\text{TA}_i(\mathbf{F}) = \text{softmax} \left( \frac{(\mathbf{W}_q(\mathbf{F} + \mathbf{m}_i^{QK}))(\mathbf{W}_k(\mathbf{F} + \mathbf{m}_i^{QK}))^T}{\sqrt{d_k}} \right) (\mathbf{W}_v(\mathbf{F} + \mathbf{m}_i^V)), \quad (3)$$

**Training** Obtaining this embedding is both efficient and convenient. Given a custom video  $x_0^{1:N}$ ,  $N$  equals to number of frames of this video, we zero-initialize each motion embedding and train the video diffusion model and backpropagate the gradient to the motion embedding:

$$\mathcal{M}_* = \arg \min_{\mathcal{M}} \mathbb{E}_{t, \epsilon} \left[ \|\epsilon_t^{1:N} - \epsilon_\theta(x_t^{1:N}, t, \mathcal{M})\|_2^2 \right], \quad (4)$$

where  $\epsilon_t$  represents the noise variable at time step  $t$ , and  $\epsilon_\theta$  denotes the noise prediction from the pre-trained video diffusion model parameterized by  $\theta$ . The whole process is shown in Figure 3. Our method also supports the loss formulation of (Jeong et al., 2023) and (Zhao et al., 2023), while the latter we found in the experiment can boost our performance too.

**Inference** During inference time, we apply a differencing operation to modify the optimized motion value embedding and debias the appearance:

$$\tilde{\mathbf{m}}_i^V[:, j, :] = \begin{cases} \mathbf{m}_i^V[:, j, :], & j = 1 \\ \mathbf{m}_i^V[:, j, :] - \mathbf{m}_i^V[:, j-1, :], & j > 1 \end{cases} \quad (5)$$

### 3.3 ANALYSIS

The motivation of our approach is to fully capture the motion information from the target video without being influenced by its appearance. In this section, we analyze how  $\mathcal{M}^{QK}$  and  $\mathcal{M}^V$  is designed to achieve this.

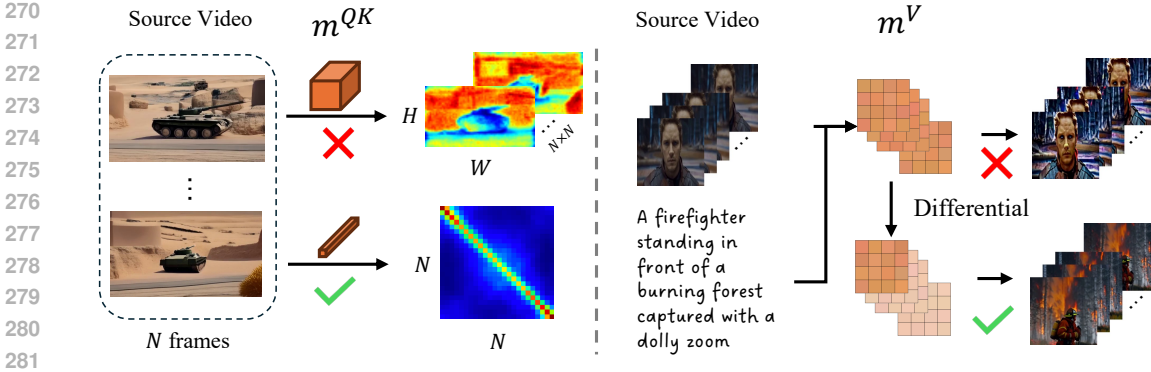


Figure 3: **Debiasing appearance from Motion Embeddings.** **Left:** For the Motion Query-Key Embedding, which influences the attention map, we exclude the spatial dimensions. Including them would cause the attention map between frames to capture the object’s shape (e.g., the shape of the tank in the original video is visible in the attention map). **Right:** Following the concept of optical flow, we apply a debias operation to the Spatial-2D Motion Value Embedding, removing static appearance and preserving dynamic motion.

**Motion Query-Key Embedding ( $\mathcal{M}^{QK}$ )** The Motion Query-Key Embedding  $\mathcal{M}^{QK}$  is designed to influence the attention map within the temporal transformer modules by adjusting the query and key components. By adding  $\mathcal{M}^{QK}$  to  $\mathbf{F}$  before the projection to queries and keys via Equation 3, we effectively modify the computation of the attention weights. These attention weights determine how frames attend to each other across time, which are critical in modeling the motion of the target video.

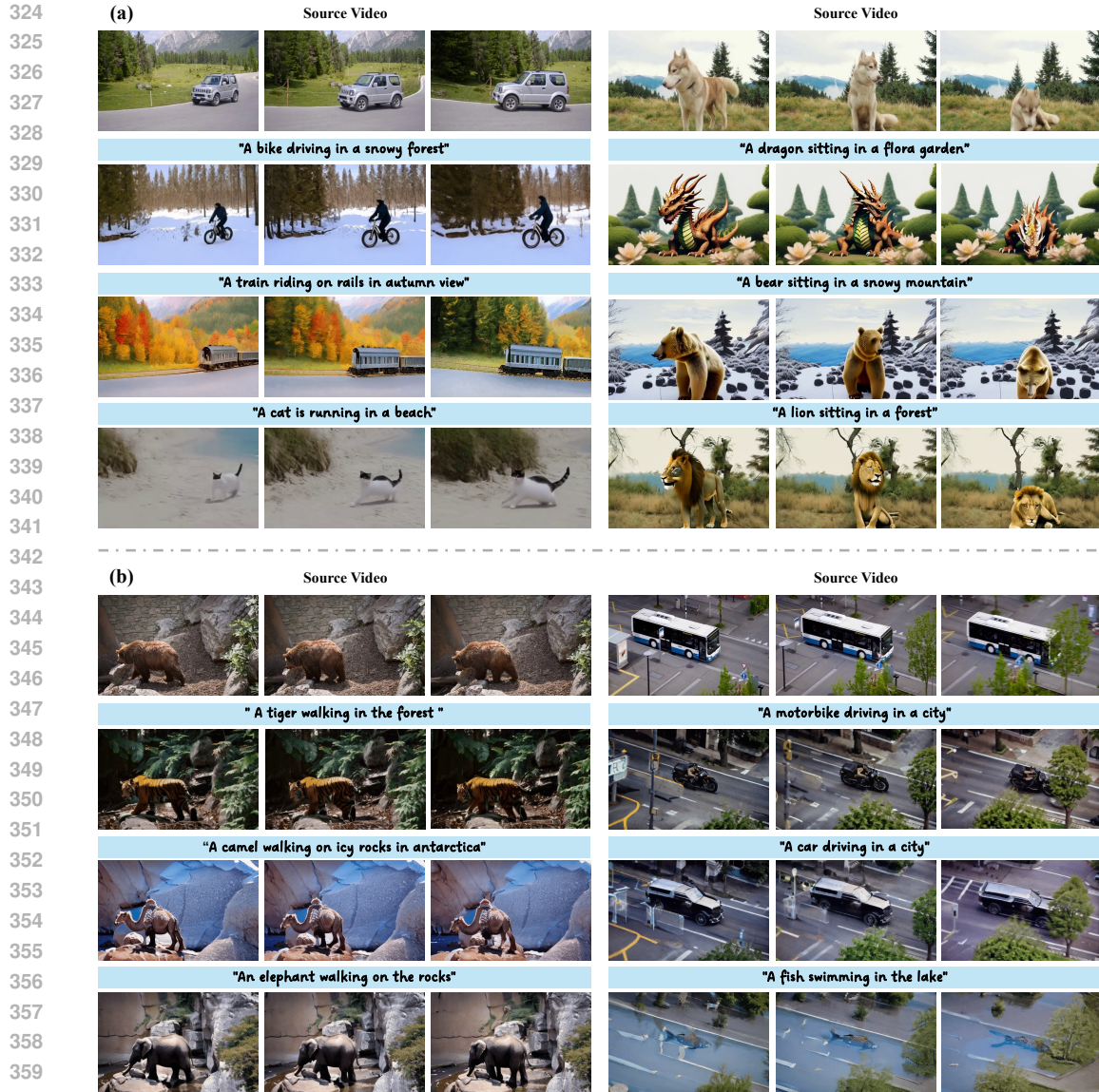
Additionally, the shape of  $\mathbf{m}_i^{QK} \in \mathbb{R}^{1 \times N \times C}$  is designed to exclude spatial dimensions ( $H$  and  $W$ ), which is crucial for removing appearance information. The rationale behind this is that the temporal attention map models the relationships between spatial regions across frames, inherently carrying the appearance information of objects. The temporal attention map has a shape of  $(H \times W) \times N \times N$ . By examining any one of the attention maps, which has the shape  $H \times W$ , the object’s shape becomes apparent, as illustrated in Figure 3. If  $\mathbf{m}_i^{QK}$  included spatial dimensions, appearance details would be captured in the embedding, limiting the ability to transfer motion to new content.

**Motion Value Embedding ( $\mathcal{M}^V$ )** As  $\mathcal{M}^{QK}$  excludes spatial dimensions, it is better suited for representing global motion (e.g., camera motion) but is less effective at capturing local motion (e.g., instance motion). To address this, we incorporate the Motion Value Embedding  $\mathcal{M}^V$  in our representation. Specifically,  $\mathbf{m}_i^V \in \mathbb{R}^{(H \times W) \times N \times C}$  includes spatial dimensions, allowing the embedding to represent motion at each spatial location across time frames. This fine-grained representation is essential for modeling local object movements and detailed motion information, enhancing the realism and coherence of the generated videos.

However,  $\mathcal{M}^V$  may capture static appearance information, leading to overfitting and limiting generalization. To address this, we apply the differencing operation from Equation 5, which isolates dynamic motion by subtracting the motion value embedding of the previous frame from the current one, removing static appearance. This approach, similar to optical flow, ensures  $\mathcal{M}^V$  focuses on motion dynamics, improving generalization to novel text prompts.

## 4 EXPERIMENT

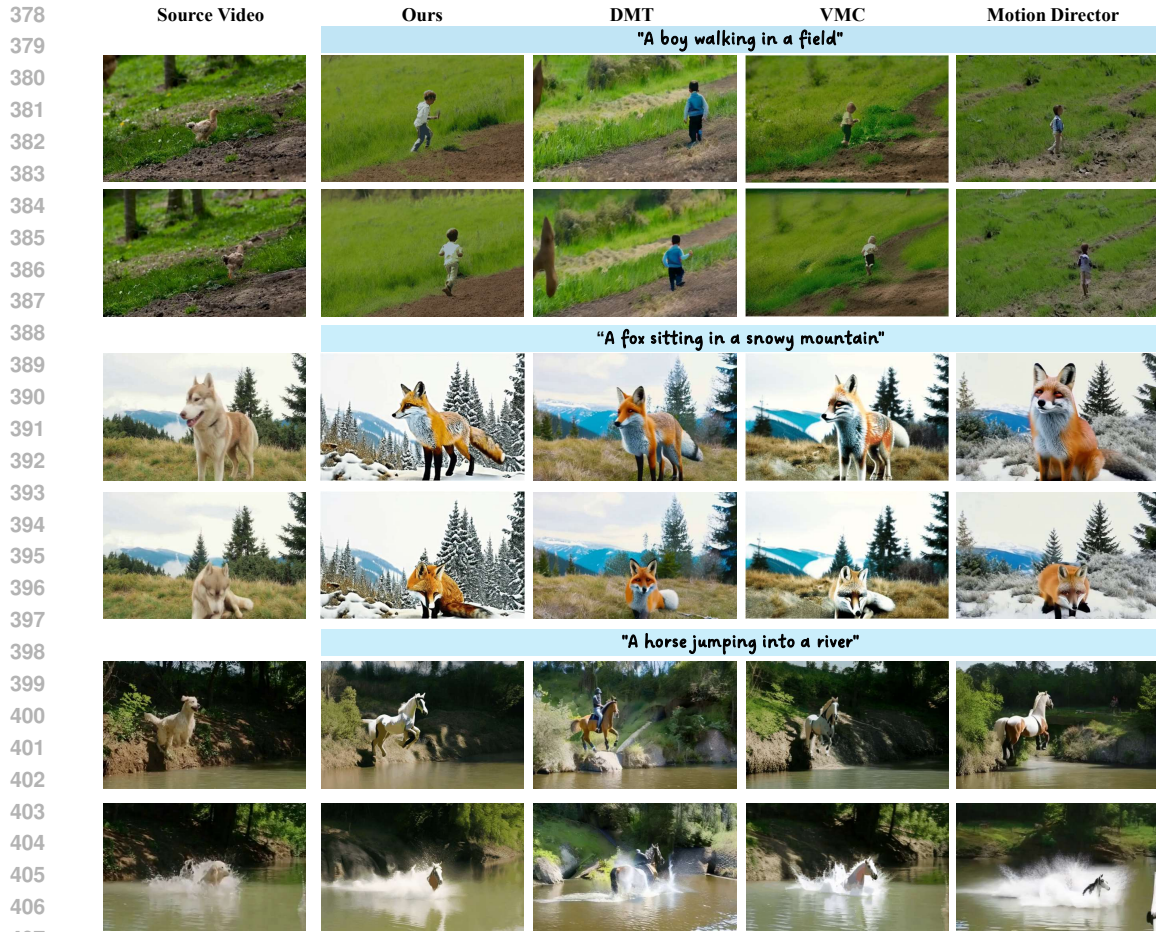
In this section, we employ three **motion customization methods** as our baselines: Diffusion Motion Transfer - CVPR24 (DMT) (Yatim et al., 2023), Video Motion Customization - CVPR24 (VMC) (Jeong et al., 2023), and Motion Director (Zhao et al., 2023). For discussions with **video editing method**, please refer to the supplementary files. To ensure a fair comparison, both our approach and the baseline methods are integrated with the same T2V model, ZeroScope (cerspense, 2023) in all experiments.



361 **Figure 4: Sample results of our method.** Our framework demonstrates exceptional adaptability in  
 362 capturing a broad spectrum of movements, accurately representing everything from subtle gestures  
 363 to intricate dynamic actions across various source videos. It also exhibits remarkable flexibility in  
 364 responding to diverse textual prompts, enabling users to guide the synthesis process with descriptive  
 365 language for customized motion outputs. Furthermore, our method seamlessly integrates with a  
 366 range of T2V models such as (a) zero-scope (cerspense, 2023) and (b) animate-diff (Guo et al.,  
 367 2023), showcasing its effectiveness in enhancing video generation with contextually rich and varied  
 368 motion patterns.

369  
370  
371  
372  
373  
374  
375  
376  
377

To be consistent with prior work (Yatim et al., 2023; Jeong et al., 2023), our evaluation utilizes  
 source videos from the DAVIS dataset (Perazzi et al., 2016), WebVID (Bain et al., 2021), and var-  
 ious online resources. These videos represent a wide range of scenes and object categories and  
 include a variety of motion types. Comprehensive details on the validation set, prompts used, and  
 implementation specifics of both our method and the baselines are provided in the Supplementary  
 files. Figure 4 showcases examples of our method in action, illustrating its proficiency in managing  
 substantial alterations to the form and structure of deforming objects while preserving the integrity  
 of the original camera and object movements.



408 Figure 5: **Qualitative results.** Compared to DMT (Yatim et al., 2023), VMC (Jeong et al., 2023),  
 409 and Motion Director (Zhao et al., 2023), our method not only preserves the original video’s motion  
 410 trajectory and object poses but also generates visual features that align with text descriptions.

#### 411 412 413 414 4.1 QUALITATIVE EVALUATION

415 As illustrated in Figure 5, our method offers a qualitative enhancement over baseline approaches. It  
 416 excels in preserving the motion trajectory and the object poses of the original video, as evidenced by  
 417 the consistent positioning and posture of objects between the initial and final frames. Additionally,  
 418 our technique demonstrates remarkable precision in generating visual features that are congruent  
 419 with textual descriptions. For instance, in the scenario “a boy walking in a field”, our model adeptly  
 420 transforms a “walking duck” into a “walking boy”, while preserving the original movement trajec-  
 421 tory. In another instance, “a fox sitting in a snowy mountain”, our approach adeptly embodies the  
 422 essence of a snow-capped mountain scene with high motion fidelity. In contrast, while Motion Di-  
 423 rector (Zhao et al., 2023) is capable of producing similar visual features of the snowy mountain, it  
 424 does not maintain the motion integrity of the original video as effectively as our method.

#### 425 426 427 4.2 QUANTITATIVE EVALUATION

428 To thoroughly evaluate our method against baselines, we conducted assessments across multiple  
 429 dimensions:

430 **Text Similarity.** Following the precedent set by previous research (Geyer et al., 2023; Esser et al.,  
 431 2023; Jeong et al., 2023; Yatim et al., 2023), we utilize CLIP (Radford et al., 2021) to assess frame-



Method	Text Similarity $\uparrow$	Motion Fidelity $\uparrow$	Temporal Consistency $\uparrow$	FID $\downarrow$	User Preference $\uparrow$
DMT (Yatim et al., 2023)	0.2883	0.7879	0.9357	614.21	16.19%
VMC (Jeong et al., 2023)	0.2707	0.9372	<b>0.9448</b>	695.97	17.18%
MD (Zhao et al., 2023)	0.3042	0.9391	0.9330	614.07	27.27%
<b>Ours</b>	<b>0.3113</b>	<b>0.9552</b>	0.9354	<b>550.38</b>	<b>39.35%</b>

Table 1: Quantitative comparisons with existing methods.

to-text similarity, calculating the average score to determine the accuracy of the edits in reflecting the intended textual modifications.

**Motion Fidelity.** To evaluate motion transfer effectiveness, we employ the Motion Fidelity Score introduced by (Yatim et al., 2023). This metric, which utilizes tracklets computed by an off-the-shelf tracking model (Karaev et al., 2023), measures the similarity between the motion trajectories in the unaligned videos, thus assessing how faithfully the output retains the input’s motion dynamics. The Motion Fidelity Score is defined as:

$$\frac{1}{m} \sum_{\tau \in \mathcal{T}} \max_{\tilde{\tau} \in \tilde{\mathcal{T}}} \text{corr}(\tau, \tilde{\tau}) + \frac{1}{n} \sum_{\tau \in \mathcal{T}} \max_{\tilde{\tau} \in \tilde{\mathcal{T}}} \text{corr}(\tau, \tilde{\tau}), \quad (6)$$

where  $\text{corr}(\tau, \tilde{\tau})$  indicates the normalized cross-correlation between tracklets  $\tau$  from the input and  $\tilde{\tau}$  from the output.

Those metrics above are considered for evaluating motion transfer tasks: conformance to the motion of the source video and the depiction of the appearance described by the text prompts. In addition to these primary metrics, quality evaluation is also conducted.

**Temporal Consistency.** Temporal consistency is widely used in video editing tasks to measure the smoothness and coherence of a video sequence (Jeong et al., 2023; Zhao et al., 2023; Kahatapitiya et al., 2024; Wu et al., 2023; Chen et al., 2023b). It is quantified by computing the average cosine similarity between the CLIP image features of all frame pairs within the output video.

**Fréchet Inception Distance (FID).** The Fréchet Inception Distance (FID), widely recognized for measuring the quality of images produced by generative models (Heusel et al., 2017), is applied in our study. In our case, images derived from a selection of 89 videos from the DAVIS dataset (Perazzi et al., 2016) are used as the reference set.

**User Study.** To rigorously evaluate our method’s effectiveness, we designed a user study that involved **121** participants. They were presented with 10 randomly selected source videos paired with corresponding text prompts, creating **10** unique scenarios that test the versatility of our approach under varied conditions. For each scenario, participants were shown a set of 4 videos, each generated by a different method but under the same conditions of motion and text prompts. The survey specifically asked participants to identify the video that best conformed to the combination of the source video’s motion and the textual description provided.

Table 1 presents a summary of the results for each metric. Evaluations were performed on a set of **66** video-edit text pairs, comprising **22** unique videos, for all metrics except user preferences. Both our method and Motion Director (Zhao et al., 2023) scored highly in text similarity. However, our approach surpassed Motion Director in motion fidelity, reinforcing the findings of the qualitative analysis. With respect to video quality, our method demonstrated a slight lag in temporal consistency when compared to VMC (Jeong et al., 2023), attributable to a lesser number of parameters. Nonetheless, in terms of individual frame quality, VMC was the least effective, significantly underperforming compared to our method. In the user study, our approach garnered a preference rate of 39.35%, the highest among the four methods evaluated, which further substantiates our method’s proficiency in preserving the original video’s motion and responding to text prompts.

### 4.3 ABLATION STUDY

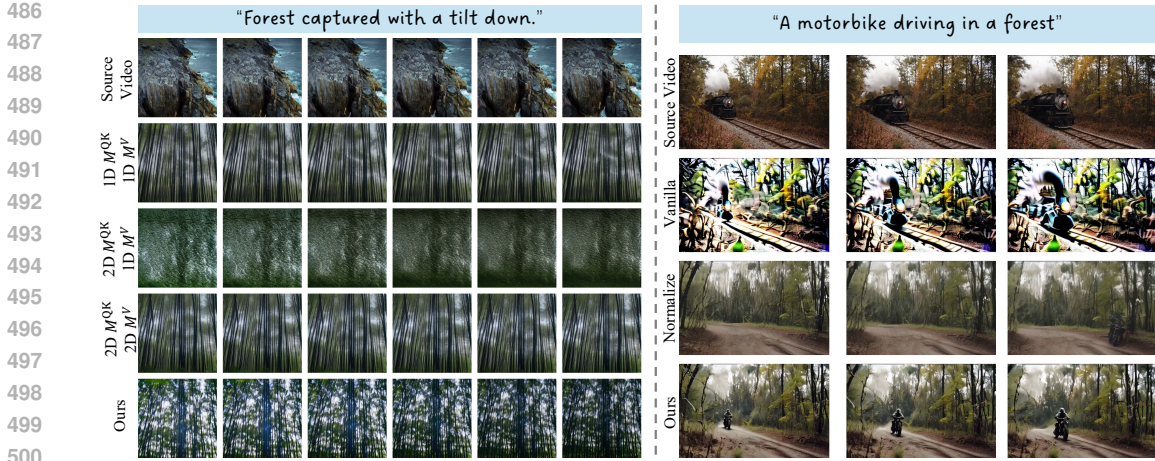


Figure 7: **Visual Result of the Ablation Study.** Left: Ablation of motion embedding design; Right: Ablation of inference strategy. **For better visualization, refer to the videos in the supplementary files.**

We conducted an ablation study of our method from two key perspectives: the design of motion embeddings and the inference strategy. For the **motion embedding design**, we evaluated three configurations: **(a)** spatial-1D  $\mathbf{m}_i^{QK}$  with spatial-1D  $\mathbf{m}_i^V$ , **(b)** spatial-2D  $\mathbf{m}_i^{QK}$  with spatial-1D  $\mathbf{m}_i^V$ , **(c)** ours, and **(d)** spatial-2D  $\mathbf{m}_i^{QK}$  with spatial-2D  $\mathbf{m}_i^V$ . For the **inference strategy**, we compared our results with two approaches: **(e)** normalize, which reduces the mean value from  $\mathbf{m}_i^V$ , and **(f)** vanilla, which does not use the debias operation defined in Equation 5. The results are shown in Figure 6. The results demonstrate that our motion embedding design achieves a strong balance between capturing the motion of the original videos and generalizing well to diverse text prompts, reducing overfitting. Furthermore, after adopting our inference strategy, the text-to-video similarity is significantly improved.

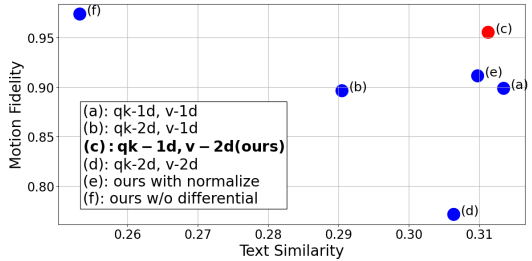


Figure 6: **Ablation Study.**

#### 4.4 LIMITATIONS

Our performance relies on the generative priors acquired by the T2V model. Consequently, the interplay between a specific target object and the motion in the input video may occasionally fall outside the T2V model’s training distribution. On the other hand, our method may encounter challenges when the input video contains interfering motions from multiple objects, as this can affect the quality of our motion embedding. This is because we learn the overall motion from the entire video rather than focusing on the motion of a specific instance. Addressing this limitation by isolating instance-level motion is a potential area for future improvement.

### 5 CONCLUSION

In conclusion, we presented a novel approach to motion customization in video generation, addressing the challenge of motion representation in generative models. Our Motion Embeddings efficiently capture both global and spatial motion while preserving temporal coherence. Additionally, our inference strategy ensures motion-focused customization by removing appearance influences. Extensive experiments demonstrate the effectiveness of our method, providing a strong foundation for future advancements in instance-level motion learning.

## REFERENCES

- 540  
541  
542 Max Bain, Arsha Nagrani, Gül Varol, and Andrew Zisserman. Frozen in time: A joint video and  
543 image encoder for end-to-end retrieval. In *Proceedings of the IEEE/CVF International Conference*  
544 *on Computer Vision*, pp. 1728–1738, 2021.
- 545 Omer Bar-Tal, Dolev Ofri-Amar, Rafail Fridman, Yoni Kasten, and Tali Dekel. Text2live: Text-  
546 driven layered image and video editing. In *European conference on computer vision*, pp. 707–723.  
547 Springer, 2022.
- 548 James Betker, Gabriel Goh, Li Jing, Tim Brooks, Jianfeng Wang, Linjie Li, Long Ouyang, Juntang  
549 Zhuang, Joyce Lee, Yufei Guo, et al. Improving image generation with better captions. *Computer*  
550 *Science*. <https://cdn.openai.com/papers/dall-e-3.pdf>, 2(3):8, 2023.
- 551  
552 Mingdeng Cao, Xintao Wang, Zhongang Qi, Ying Shan, Xiaohu Qie, and Yinqiang Zheng. Mas-  
553 actrl: Tuning-free mutual self-attention control for consistent image synthesis and editing. *arXiv*  
554 *preprint arXiv:2304.08465*, 2023.
- 555 cerspense. zeroscope\_v2. [https://huggingface.co/cerspense/zeroscope\\_v2\\_](https://huggingface.co/cerspense/zeroscope_v2_576w)  
556 [576w](https://huggingface.co/cerspense/zeroscope_v2_576w), 2023. Accessed: 2023-02-03.
- 557  
558 Hila Chefer, Yuval Alaluf, Yael Vinker, Lior Wolf, and Daniel Cohen-Or. Attend-and-excite:  
559 Attention-based semantic guidance for text-to-image diffusion models. *ACM Transactions on*  
560 *Graphics (TOG)*, 42(4):1–10, 2023.
- 561  
562 Haoxin Chen, Menghan Xia, Yingqing He, Yong Zhang, Xiaodong Cun, Shaoshu Yang, Jinbo Xing,  
563 Yaofang Liu, Qifeng Chen, Xintao Wang, et al. Videocrafter1: Open diffusion models for high-  
564 quality video generation. *arXiv preprint arXiv:2310.19512*, 2023a.
- 565  
566 Haoxin Chen, Yong Zhang, Xiaodong Cun, Menghan Xia, Xintao Wang, Chao Weng, and Ying  
567 Shan. Videocrafter2: Overcoming data limitations for high-quality video diffusion models. *arXiv*  
568 *preprint arXiv:2401.09047*, 2024.
- 569  
570 Weifeng Chen, Jie Wu, Pan Xie, Hefeng Wu, Jiashi Li, Xin Xia, Xuefeng Xiao, and Liang Lin.  
571 Control-a-video: Controllable text-to-video generation with diffusion models. *arXiv preprint*  
572 *arXiv:2305.13840*, 2023b.
- 573  
574 Patrick Esser, Johnathan Chiu, Parmida Atighehchian, Jonathan Granskog, and Anastasis Germani-  
575 dis. Structure and content-guided video synthesis with diffusion models. In *Proceedings of the*  
576 *IEEE/CVF International Conference on Computer Vision*, pp. 7346–7356, 2023.
- 577  
578 Rinon Gal, Yuval Alaluf, Yuval Atzmon, Or Patashnik, Amit H Bermano, Gal Chechik, and Daniel  
579 Cohen-Or. An image is worth one word: Personalizing text-to-image generation using textual  
580 inversion. *arXiv preprint arXiv:2208.01618*, 2022.
- 581  
582 Michal Geyer, Omer Bar-Tal, Shai Bagon, and Tali Dekel. Tokenflow: Consistent diffusion features  
583 for consistent video editing. *arXiv preprint arXiv:2307.10373*, 2023.
- 584  
585 Yuwei Guo, Ceyuan Yang, Anyi Rao, Yaohui Wang, Yu Qiao, Dahua Lin, and Bo Dai. Animatediff:  
586 Animate your personalized text-to-image diffusion models without specific tuning. *arXiv preprint*  
587 *arXiv:2307.04725*, 2023.
- 588  
589 Hao He, Yinghao Xu, Yuwei Guo, Gordon Wetzstein, Bo Dai, Hongsheng Li, and Ceyuan  
590 Yang. Cameractrl: Enabling camera control for text-to-video generation. *arXiv preprint*  
591 *arXiv:2404.02101*, 2024.
- 592  
593 Yingqing He, Tianyu Yang, Yong Zhang, Ying Shan, and Qifeng Chen. Latent video diffusion mod-  
594 els for high-fidelity video generation with arbitrary lengths. *arXiv preprint arXiv:2211.13221*,  
595 2022.
- 596  
597 Amir Hertz, Ron Mokady, Jay Tenenbaum, Kfir Aberman, Yael Pritch, and Daniel Cohen-Or.  
598 Prompt-to-prompt image editing with cross attention control. *arXiv preprint arXiv:2208.01626*,  
599 2022.

- 594 Martin Heusel, Hubert Ramsauer, Thomas Unterthiner, Bernhard Nessler, and Sepp Hochreiter.  
595 Gans trained by a two time-scale update rule converge to a local nash equilibrium. *Advances in*  
596 *neural information processing systems*, 30, 2017.
- 597  
598 Wenyi Hong, Ming Ding, Wendi Zheng, Xinghan Liu, and Jie Tang. Cogvideo: Large-scale pre-  
599 training for text-to-video generation via transformers. *arXiv preprint arXiv:2205.15868*, 2022.
- 600 Edward J Hu, Yelong Shen, Phillip Wallis, Zeyuan Allen-Zhu, Yanzhi Li, Shean Wang, Lu Wang,  
601 and Weizhu Chen. Lora: Low-rank adaptation of large language models. *arXiv preprint*  
602 *arXiv:2106.09685*, 2021.
- 603  
604 Hyeonho Jeong, Geon Yeong Park, and Jong Chul Ye. Vmc: Video motion customization using  
605 temporal attention adaption for text-to-video diffusion models. *arXiv preprint arXiv:2312.00845*,  
606 2023.
- 607  
608 Hyeonho Jeong, Jinho Chang, Geon Yeong Park, and Jong Chul Ye. Dreammotion: Space-time  
609 self-similarity score distillation for zero-shot video editing. *arXiv preprint arXiv:2403.12002*,  
610 2024.
- 611 Kumara Kahatapitiya, Adil Karjauv, Davide Abati, Fatih Porikli, Yuki M Asano, and Amirhossein  
612 Habibian. Object-centric diffusion for efficient video editing. *arXiv preprint arXiv:2401.05735*,  
613 2024.
- 614 Nikita Karaev, Ignacio Rocco, Benjamin Graham, Natalia Neverova, Andrea Vedaldi, and Christian  
615 Rupprecht. Cotracker: It is better to track together. *arXiv preprint arXiv:2307.07635*, 2023.
- 616  
617 Guillaume Le Moing, Jean Ponce, and Cordelia Schmid. Ccvs: context-aware controllable video  
618 synthesis. *Advances in Neural Information Processing Systems*, 34:14042–14055, 2021.
- 619  
620 Yitong Li, Martin Min, Dinghan Shen, David Carlson, and Lawrence Carin. Video generation from  
621 text. In *Proceedings of the AAAI conference on artificial intelligence*, volume 32, 2018.
- 622  
623 Jun Hao Liew, Hanshu Yan, Jianfeng Zhang, Zhongcong Xu, and Jiashi Feng. Magicedit: High-  
624 fidelity and temporally coherent video editing. *arXiv preprint arXiv:2308.14749*, 2023.
- 625  
626 Pengyang Ling, Jiazi Bu, Pan Zhang, Xiaoyi Dong, Yuhang Zang, Tong Wu, Huaian Chen, Jiaqi  
627 Wang, and Yi Jin. Motionclone: Training-free motion cloning for controllable video generation.  
628 *arXiv preprint arXiv:2406.05338*, 2024.
- 629  
630 Shaoteng Liu, Yuechen Zhang, Wenbo Li, Zhe Lin, and Jiaya Jia. Video-p2p: Video editing with  
631 cross-attention control. *arXiv preprint arXiv:2303.04761*, 2023.
- 632  
633 Wan-Duo Kurt Ma, John P Lewis, and W Bastiaan Kleijn. Trailblazer: Trajectory control for  
634 diffusion-based video generation. *arXiv preprint arXiv:2401.00896*, 2023a.
- 635  
636 Wan-Duo Kurt Ma, JP Lewis, W Bastiaan Kleijn, and Thomas Leung. Directed diffusion: Direct  
637 control of object placement through attention guidance. *arXiv preprint arXiv:2302.13153*, 2023b.
- 638  
639 Chenlin Meng, Yutong He, Yang Song, Jiaming Song, Jiajun Wu, Jun-Yan Zhu, and Stefano Ermon.  
640 Sdedit: Guided image synthesis and editing with stochastic differential equations. *arXiv preprint*  
641 *arXiv:2108.01073*, 2021.
- 642  
643 Chong Mou, Xintao Wang, Liangbin Xie, Jian Zhang, Zhongang Qi, Ying Shan, and Xiaohu Qie.  
644 T2i-adapter: Learning adapters to dig out more controllable ability for text-to-image diffusion  
645 models. *arXiv preprint arXiv:2302.08453*, 2023.
- 646  
647 Alex Nichol, Prafulla Dhariwal, Aditya Ramesh, Pranav Shyam, Pamela Mishkin, Bob McGrew,  
Ilya Sutskever, and Mark Chen. Glide: Towards photorealistic image generation and editing with  
text-guided diffusion models. *arXiv preprint arXiv:2112.10741*, 2021.
- Yingwei Pan, Zhaofan Qiu, Ting Yao, Houqiang Li, and Tao Mei. To create what you tell: Generat-  
ing videos from captions. In *Proceedings of the 25th ACM international conference on Multime-  
dia*, pp. 1789–1798, 2017.

- 648 Or Patashnik, Daniel Garibi, Idan Azuri, Hadar Averbuch-Elor, and Daniel Cohen-Or. Lo-  
649 calizing object-level shape variations with text-to-image diffusion models. *arXiv preprint*  
650 *arXiv:2303.11306*, 2023.
- 651 Federico Perazzi, Jordi Pont-Tuset, Brian McWilliams, Luc Van Gool, Markus Gross, and Alexander  
652 Sorkine-Hornung. A benchmark dataset and evaluation methodology for video object segmen-  
653 tation. In *Proceedings of the IEEE conference on computer vision and pattern recognition*, pp.  
654 724–732, 2016.
- 655 Chenyang Qi, Xiaodong Cun, Yong Zhang, Chenyang Lei, Xintao Wang, Ying Shan, and Qifeng  
656 Chen. Fatezero: Fusing attentions for zero-shot text-based video editing. *arXiv preprint*  
657 *arXiv:2303.09535*, 2023.
- 658 Alec Radford, Jong Wook Kim, Chris Hallacy, Aditya Ramesh, Gabriel Goh, Sandhini Agarwal,  
659 Girish Sastry, Amanda Askell, Pamela Mishkin, Jack Clark, et al. Learning transferable visual  
660 models from natural language supervision. In *International conference on machine learning*, pp.  
661 8748–8763. PMLR, 2021.
- 662 Aditya Ramesh, Prafulla Dhariwal, Alex Nichol, Casey Chu, and Mark Chen. Hierarchical text-  
663 conditional image generation with clip latents. *arXiv preprint arXiv:2204.06125*, 2022.
- 664 Robin Rombach, Andreas Blattmann, Dominik Lorenz, Patrick Esser, and Björn Ommer. High-  
665 resolution image synthesis with latent diffusion models. In *Proceedings of the IEEE/CVF confer-*  
666 *ence on computer vision and pattern recognition*, pp. 10684–10695, 2022.
- 667 Nataniel Ruiz, Yuanzhen Li, Varun Jampani, Yael Pritch, Michael Rubinstein, and Kfir Aberman.  
668 Dreambooth: Fine tuning text-to-image diffusion models for subject-driven generation. In *Pro-*  
669 *ceedings of the IEEE/CVF Conference on Computer Vision and Pattern Recognition*, pp. 22500–  
670 22510, 2023.
- 671 Chitwan Saharia, William Chan, Saurabh Saxena, Lala Li, Jay Whang, Emily L Denton, Kamyar  
672 Ghasemipour, Raphael Gontijo Lopes, Burcu Karagol Ayan, Tim Salimans, et al. Photorealistic  
673 text-to-image diffusion models with deep language understanding. *Advances in Neural Informa-*  
674 *tion Processing Systems*, 35:36479–36494, 2022.
- 675 Masaki Saito, Eiichi Matsumoto, and Shunta Saito. Temporal generative adversarial nets with sin-  
676 gular value clipping. In *Proceedings of the IEEE international conference on computer vision*,  
677 pp. 2830–2839, 2017.
- 678 Aliaksandr Siarohin, Stéphane Lathuilière, Sergey Tulyakov, Elisa Ricci, and Nicu Sebe. Animat-  
679 ing arbitrary objects via deep motion transfer. In *Proceedings of the IEEE/CVF Conference on*  
680 *Computer Vision and Pattern Recognition*, pp. 2377–2386, 2019a.
- 681 Aliaksandr Siarohin, Stéphane Lathuilière, Sergey Tulyakov, Elisa Ricci, and Nicu Sebe. First order  
682 motion model for image animation. *Advances in neural information processing systems*, 32,  
683 2019b.
- 684 Uriel Singer, Adam Polyak, Thomas Hayes, Xi Yin, Jie An, Songyang Zhang, Qiyuan Hu, Harry  
685 Yang, Oron Ashual, Oran Gafni, et al. Make-a-video: Text-to-video generation without text-video  
686 data. *arXiv preprint arXiv:2209.14792*, 2022.
- 687 Kihyuk Sohn, Nataniel Ruiz, Kimin Lee, Daniel Castro Chin, Irina Blok, Huiwen Chang, Jarred  
688 Barber, Lu Jiang, Glenn Entis, Yuanzhen Li, et al. Styledrop: Text-to-image generation in any  
689 style. *arXiv preprint arXiv:2306.00983*, 2023.
- 690 Yu Tian, Jian Ren, Menglei Chai, Kyle Olszewski, Xi Peng, Dimitris N Metaxas, and Sergey  
691 Tulyakov. A good image generator is what you need for high-resolution video synthesis. *arXiv*  
692 *preprint arXiv:2104.15069*, 2021.
- 693 Narek Tumanyan, Michal Geyer, Shai Bagon, and Tali Dekel. Plug-and-play diffusion features for  
694 text-driven image-to-image translation. In *Proceedings of the IEEE/CVF Conference on Com-*  
695 *puter Vision and Pattern Recognition*, pp. 1921–1930, 2023.

- 702 Carl Vondrick, Hamed Pirsiavash, and Antonio Torralba. Generating videos with scene dynamics.  
703 *Advances in neural information processing systems*, 29, 2016.  
704
- 705 Jiuniu Wang, Hangjie Yuan, Dayou Chen, Yingya Zhang, Xiang Wang, and Shiwei Zhang. Mod-  
706 elscape text-to-video technical report. *arXiv preprint arXiv:2308.06571*, 2023.
- 707 Zhouxia Wang, Ziyang Yuan, Xintao Wang, Yaowei Li, Tianshui Chen, Menghan Xia, Ping Luo,  
708 and Ying Shan. Motionctrl: A unified and flexible motion controller for video generation. In  
709 *ACM SIGGRAPH 2024 Conference Papers*, pp. 1–11, 2024.  
710
- 711 Chenfei Wu, Jian Liang, Lei Ji, Fan Yang, Yuejian Fang, Daxin Jiang, and Nan Duan. Nüwa: Visual  
712 synthesis pre-training for neural visual world creation. In *European conference on computer*  
713 *vision*, pp. 720–736. Springer, 2022.
- 714 Jay Zhangjie Wu, Yixiao Ge, Xintao Wang, Stan Weixian Lei, Yuchao Gu, Yufei Shi, Wynne Hsu,  
715 Ying Shan, Xiaohu Qie, and Mike Zheng Shou. Tune-a-video: One-shot tuning of image diffusion  
716 models for text-to-video generation. In *Proceedings of the IEEE/CVF International Conference*  
717 *on Computer Vision*, pp. 7623–7633, 2023.
- 718 Wilson Yan, Yunzhi Zhang, Pieter Abbeel, and Aravind Srinivas. Videogpt: Video generation using  
719 vq-vae and transformers. *arXiv preprint arXiv:2104.10157*, 2021.  
720
- 721 Danah Yatim, Rafail Fridman, Omer Bar Tal, Yoni Kasten, and Tali Dekel. Space-time diffusion  
722 features for zero-shot text-driven motion transfer. *arXiv preprint arXiv:2311.17009*, 2023.  
723
- 724 Hu Ye, Jun Zhang, Sibao Liu, Xiao Han, and Wei Yang. Ip-adapter: Text compatible image prompt  
725 adapter for text-to-image diffusion models. *arXiv preprint arXiv:2308.06721*, 2023.
- 726 Shengming Yin, Chenfei Wu, Jian Liang, Jie Shi, Houqiang Li, Gong Ming, and Nan Duan. Drag-  
727 nuwa: Fine-grained control in video generation by integrating text, image, and trajectory. *arXiv*  
728 *preprint arXiv:2308.08089*, 2023.
- 729 David Junhao Zhang, Jay Zhangjie Wu, Jia-Wei Liu, Rui Zhao, Lingmin Ran, Yuchao Gu, Difei  
730 Gao, and Mike Zheng Shou. Show-1: Marrying pixel and latent diffusion models for text-to-  
731 video generation. *arXiv preprint arXiv:2309.15818*, 2023.  
732
- 733 David Junhao Zhang, Dongxu Li, Hung Le, Mike Zheng Shou, Caiming Xiong, and Doyen Sahoo.  
734 Moonshot: Towards controllable video generation and editing with multimodal conditions. *arXiv*  
735 *preprint arXiv:2401.01827*, 2024.
- 736 Lvmin Zhang and Maneesh Agrawala. Adding conditional control to text-to-image diffusion models.  
737 *arXiv preprint arXiv:2302.05543*, 2023.  
738
- 739 Rui Zhao, Yuchao Gu, Jay Zhangjie Wu, David Junhao Zhang, Jiawei Liu, Weijia Wu, Jussi Keppo,  
740 and Mike Zheng Shou. Motiondirector: Motion customization of text-to-video diffusion models.  
741 *arXiv preprint arXiv:2310.08465*, 2023.  
742  
743  
744  
745  
746  
747  
748  
749  
750  
751  
752  
753  
754  
755